Organic matter from redoximorphic soils accelerates and sustains microbial Fe(III) reduction

Journal:	*Environmental Science & Technology*
Manuscript ID	es-2021-01183k.R3
Manuscript Type:	Article
Date Submitted by the Author:	30-Jun-2021
Complete List of Authors:	Fritzsche, Andreas; Friedrich Schiller University Jena, Institute of Geosciences; Intrapore GmbH Bosch, Julian; Helmholtz Zentrum Munchen Deutsches Forschungszentrum fur Gesundheit und Umwelt, Institute of Groundwater Ecology; Intrapore GmbH Sander, Michael; Eidgenossische Technische Hochschule Zurich, Environmental Sciences Schröder, Christian; University of Stirling, Biological and Environmental Sciences Byrne, James; Eberhard Karls Universitat Tubingen, Department of Geosciences; University of Bristol, School of Earth Sciences Ritschel, Thomas; Friedrich-Schiller-Universitat Jena, Institute of Geosciences Joshi, Prachi; Eberhard Karls Universitat Tubingen, Department of Geosciences Maisch, Markus; Eberhard Karls Universitat Tubingen Fachbereich III Geowissenschaften, Meckenstock, Rainer; Helmholtz Center Munich German Research Center for Environmental Health, Institute of Groundwater Ecology; University of Duisburg-Essen, Biofilm Centre Kappler, Andreas; Eberhard Karls Universitat Tubingen, Center for Applied Geosciences Totsche, Kai; Friedrich-Schiller-Universitat Jena, Institute of Geosciences

Organic matter from redoximorphic soils accelerates and sustains microbial Fe(III) reduction

Andreas Fritzsche [a,1,*], *Julian Bosch* [b,1], *Michael Sander* [c], *Christian Schröder* [d], *James M. Byrne* [e,2], *Thomas Ritschel* [a], *Prachi Joshi* [e], *Markus Maisch* [e], *Rainer U. Meckenstock* [b,3], *Andreas Kappler* [e], *Kai U. Totsche* [a]

[a] Institute of Geosciences, Friedrich-Schiller-University Jena, Burgweg 11, D-07749 Jena, Germany (thomas.ritschel@uni-jena.de, kai.totsche@uni-jena.de)

[b] Institute of Groundwater Ecology, Helmholtz Centre Munich - German Research Center for Environmental Health, D-85764 Neuherberg, Germany

[c] Department of Environmental Systems Science, Institute of Biogeochemistry and Pollutant Dynamics, Swiss Federal Institute of Technology (ETH) Zurich, CH-8092 Zurich, Switzerland (michael.sander@env.ethz.ch)

[d] Biological and Environmental Sciences, Faculty of Natural Sciences, University of Stirling, Stirling FK9 4LA, UK (christian.schroeder@stir.ac.uk)

[e] Geomicrobiology, Center for Applied Geosciences, University of Tübingen, D-72076 Tübingen, Germany (prachi.joshi@uni-tuebingen.de; markus.maisch@uni-tuebingen.de; andreas.kappler@uni-tuebingen.de)

[1] present: Intrapore GmbH, D-45327 Essen, Germany (julian.bosch@intrapore.com)

[2] present: School of Earth Sciences, Bristol BS8 1RJ, UK (james.byrne@bristol.ac.uk)

[3] present: Environmental Microbiology and Biotechnology, University of Duisburg-Essen, D-45141 Essen, Germany (rainer.meckenstock@uni-due.de)

* Corresponding author. Tel.: +49 3641 948 715; fax: +49 3641 948 742; a.fritzsche@uni-jena.de

ABSTRACT

Microbial reduction of Fe(III) minerals is a prominent process in redoximorphic soils and is strongly affected by organic matter (OM). We herein determined the rate and extent of microbial reduction of ferrihydrite (Fh) with either adsorbed or coprecipitated OM by *Geobacter sulfurreducens*. We focused on OM-mediated effects on electron uptake and alterations in Fh crystallinity. The OM was obtained from anoxic soil columns (effluent OM, efOM) and included –unlike water-extractable OM– compounds released by microbial activity under anoxic conditions. We found that organic molecules in efOM had generally no or only very low electron-accepting capacity and were incorporated into the Fh aggregates when coprecipitated with Fh. Compared to OM-free Fh, adsorption of efOM to Fh decelerated the microbial Fe(III) reduction by passivating the Fh surface towards electron uptake. In contrast, coprecipitation of Fh with efOM accelerated the microbial reduction, likely because efOM disrupted the Fh structure as noted by Mössbauer spectroscopy. Additionally, adsorbed and co-precipitated efOM resulted in a more sustained Fe(III) reduction, potentially because efOM could have effectively scavenged biogenic Fe(II) and prevented the passivation of the Fh surface by adsorbed Fe(II). Fe(III)-OM

coprecipitates forming at anoxic-oxic interfaces are thus likely readily reducible by Fe(III)-reducing bacteria in redoximorphic soils.

Synopsis

If associated with Fe oxides, mobile OM from anoxic topsoil sustains and frequently accelerates the microbial Fe(III) reduction, despite its low-to-absent capacity for electron uptake.

Keywords

Mössbauer spectroscopy, mediated electrochemical reduction, electron-accepting capacity, ferrihydrite, iron oxide, dissolved organic matter, DOM

INTRODUCTION

Microbial reduction of poorly-soluble Fe(III) to soluble Fe(II) plays an important role in the cycling of iron in circumneutral suboxic and anoxic environments.[1, 2] Numerous studies have investigated the factors determining the rate and extent of microbial Fe(III) reduction with a prominent focus on the impact of natural organic matter (OM). Apart from serving as energy

source and thereby fueling the microbial metabolism,[3-5] previous studies have provided evidence that dissolved natural OM directly affects microbial Fe(III) reduction by acting (i) as a ligand, which increases the solubility of Fe(III),[6] (ii) as a ligand for Fe(II), which helps sustain Fe(III) reduction through removal of adsorbed Fe(II) from mineral surfaces,[7] (iii) as redox-active electron-shuttling compound mediating the transfer of electrons from microbial respiration to terminal electron acceptors (iron (oxyhydr-)oxides, dissolved O_2, etc.),[8] and (iv) as an adsorbate on Fe(III) mineral surfaces, thereby blocking access for Fe(III)-reducing bacteria.[9] Natural OM can also indirectly affect the microbial Fe(III) reduction by (v) altering the crystallinity [10] and solubility [11] of iron (oxyhydr-)oxide minerals as well as (vi) their aggregate sizes,[12] which can result in diverse and partially opposing impacts depending on the Fe(III)-reducing bacteria present.[9, 13-15]

Many studies have previously confined the impact of natural OM on Fe(III) reduction in soils and sediments to humic isolates from peat, soils, or surface water. Yet, it has been subsequently established that humic substances do not necessarily reflect the properties of OM that is present in soil pore solutions.[16] Hence, approaches that capture the actual solubilization of OM in soils are gaining preference to the use of alkaline extracts, i.e. humic substances, as proxies for pedogenic OM.[17] For example, water-extractable OM from organic surface layers was recently used in Fe(III)

reduction experiments.[9, 18-20] However, it remains unclear if water-extractable OM reflects the composition of OM that occurs in (redoximorphic) soils. Water extractions typically employ i) liquid-to-solid ratios considerably exceeding those in soils, ii) agitation, iii) extraction with ultrapure water, and iv) predominantly oxic conditions. These conditions are known to preferentially extract certain fractions of OM,[21] e.g., compounds with elevated aromaticity,[22] and may also ignore OM fractions relevant for redoximorphic soils. For example, oxic conditions during extraction omit the reductive dissolution of pedogenic iron (oxyhydr-)oxides and thereby the release of OM from the minerals upon their reduction.[23] It has been shown that 72-92% of OM associated with pedogenic iron (oxyhydr-)oxides are not water-extractable,[24] thus they would not be released by conventional batch water extractions. However, this particular OM represents a likely relevant fraction for microbial Fe(III) reduction in redoximorphic soils. It may migrate through redoximorphic soils eventually encountering anoxic-oxic interfaces where it may i) coprecipitate with or adsorb to *de novo* Fe(III) minerals,[25] and/or ii) re-oxidize and serve as electron shuttles that accept electrons from microbial respiration.

Our study explores the impact of OM, which was derived from anoxic systems, on microbial Fe(III) reduction. We assessed the rate and extent of microbial reduction by *Geobacter*

sulfurreducens of organo-mineral ferrihydrite with either adsorbed or coprecipitated OM from an anoxic topsoil. Unlike water-extractable OM, the OM used in our study includes compounds released by microbial activity under anoxic conditions, e.g., OM from the dissolution of pedogenic iron (oxyhydr-)oxides. We focused on OM-mediated effects on electron transfer and mineral crystallinity rather than the potential of these C sources to serve as e^--donors for microbial Fe(III) reduction. We hypothesize that mobile OM from anoxic topsoil accepts electrons and alters ferrihydrite crystallinity, particularly during coprecipitation. We thus expect this anoxic OM to accelerate and sustain microbial Fe(III) reduction.

MATERIALS AND METHODS

Origin of soil effluent organic matter (efOM), humic acid (HA) and synthesis of ferrihydrite (Fh)

efOM: Organic matter, which is mobile under anoxic conditions, cannot be extracted entirely from intact soils due to the presence of oxic regions, despite e.g., inundation with water.[26] We therefore used a lab-based soil column setup to overcome the limitations of batch extractions with water.[27] All mobile OM eluting from anoxic soil columns is herein referred to as effluent OM

(efOM). Air-dried and <2 mm-sieved topsoil material (665±25 g; arithmetic mean ± range of two independent soil column replicates) was filled into two replicate soil columns (stainless steel; length: 15.5 cm, diameter: 9.1 cm, V=1000 cm^3) operated at 295±2 K. The soil material originated from a humus-rich topsoil horizon (Ah; Table S1) of a gleyic Fluvisol [28] from a floodplain site (Mulde river, Sachsen-Anhalt, Germany). The columns were fed via a peristaltic pump (Reglo Analog, Ismatec, Switzerland) with an oxic, low ionic influent (10^{-3} M NaCl; Merck, Germany; pH~5.6) at a nominal porewater velocity of 5.5 cm d^{-1} from bottom to top to achieve water-saturated conditions. The average contact time between liquid and solid phase during percolation was ~2.8 d. A detailed description of the percolation protocol is provided in the Supporting Information S1. Fe(III)- and SO_4^{2-}-reducing conditions were established within the soil columns due to the activity of autochthonous microbial communities and led to the reductive dissolution of pedogenic iron (oxyhydr-)oxides (Figure S1). Upon discharge from the soil column, the effluent solution was exposed to the ambient, oxic atmosphere. At a prevailing effluent pH of ~7.5 (Figure S1), this would have resulted in the formation of Fe(III)-OM coprecipitates, which form from Fe(II), which is concomitantly present in the soil solution derived from anoxic compartments.[25] Coprecipitation of OM with *de novo* Fe(III) minerals would result in a fractionation between

115 dissolved and mineral-bound OM according to its molecular composition.[29, 30] This could be
116 overcome by keeping the soil solution or soil effluent permanently under anoxic conditions until
117 dialysis, i.e., the removal of effluent Fe(II) has been completed. To deliver efOM in the required
118 quantities, ~1.8 L effluent per soil column had to be dialyzed, which required a total of 43
119 exchanges with ultrapure water (each with ~10 L). It was therefore unlikely that anoxic conditions
120 could have been maintained during the complete process of dialysis. We therefore chose the
121 following approach to retrieve the entire efOM from anoxic soil: the effluent was acidified with
122 HCl immediately after its discharge from the soil column (final concentration: 0.25 M HCl). The
123 effluent pH remained <1 by this treatment, which effectively retarded the oxidation of the effluent
124 Fe(II).[31] We did not observe any precipitation of OM (e.g., such as humic acids). The acidified
125 effluent was dialyzed to remove coincident Fe(II) and other inorganic ions (100-500 Da,
126 Spectra/Por Biotech CE, Spectrum Laboratories, USA) to prevent the precipitation of iron
127 (oxyhydr-)oxides and of salts during freeze-drying (Alpha 1-4 LSC, Christ, Germany). Although
128 the electric conductivity of the effluent dropped from ~73 mS cm^{-1} before dialysis (excess H_3O^+
129 and Cl^-) to ~40 µS cm^{-1} after dialysis, some Fe remained in the dialyzed effluent most likely as
130 nano-aggregated Fe-OM coprecipitates (Figure S2). With dialysis, the concentration of effluent Fe

131 decreased from 116±13 mg L^{-1} to 24±3 mg L^{-1}. Excitation-emission-matrices from the
132 corresponding effluent samples indicated that dialysis did not change the composition of efOM
133 except for a potential partial loss in polyphenolic substances (Figure S3). This may have resulted
134 in a dialysis-induced decrease in the electron-donating capacity of efOM. However, this property
135 is irrelevant for our microbial reduction experiments, in which the investigated OM specimens
136 (efOM, humic acids) did not act as electron donators but rather as potential electron acceptors in
137 microbial reduction. We assumed that the effects on efOM properties by the instant effluent
138 acidification were reversible when pH was raised to higher values. This assumption was supported
139 by the general reversibility of pH-induced changes in the emission-excitation-matrices of efOM
140 (Figure S3 and Table S2). Emission-excitation-matrices are sensitive to changes in OM
141 fluorophores and their molecular environment.[32]

142 *HA:* HA was obtained from anoxic OM-rich groundwater [33] (~97 mg dissolved OC L^{-1}) from a
143 different site (Gorleben, Germany) by enrichment via reverse osmosis and fractionation according
144 to the XAD-8 method.[34] Solid HA was re-dissolved and stirred (1 h) in ultrapure water at pH~10
145 (NaOH; Sigma-Aldrich, Germany). Subsequently, the solution pH was re-adjusted to pH=7 (HCl;

Merck), stirred overnight, centrifuged (30 min, 293 K, 10,000 rpm), and filtered (0.22 µm, sterile polyethersulfone, Millex-GP; Merck Millipore; Germany).

Fh: 6-line Fh was synthesized by dissolving 5 g $Fe(NO_3)_3 \times 9H_2O$ (Sigma-Aldrich) in 500 ml ultrapure water, stirring at 348 K for 12 minutes, and subsequently cooling down to room temperature in an ice bath (final pH=5.7).[35] For coprecipitation with HA, HA-solutions with 2.0, 60.5 and 184 mg OC L^{-1} were used instead of water, which corresponds to OC/Fe ratios of 0.01, 0.32 and 0.96 mol_C/mol_{Fe}, respectively, in the solutions. For coprecipitation with efOM, 1 g $Fe(NO_3)_3 \times 9H_2O$ was dissolved in 200 ml dialyzed, efOM-containing effluent from the duplicate soil columns (OC=65±1 mg L^{-1}), resulting in OC/Fe ratios of ~0.44 mol_C/mol_{Fe} in the solutions. For adsorption, OM-free Fh was stirred for 3 d in the dark in HA-solutions and in dialyzed soil effluent to obtain OC/Fe ratios of 0.01, 0.32, 0.96 (adsorbed HA) and 0.68 mol_C/mol_{Fe} (adsorbed efOM) in the solutions. With respect to effluents from anoxic soil columns,[25] these initial OC/Fe ratios were comparably low. This was chosen to prevent the formation of organic Fe(III) complexes, which is reported at higher initial OC/Fe ratios.[36] Organically complexed Fe(III) is distinctly more available for microbial reduction,[37] and could therefore mask any effects by OM-mediated alterations in Fh crystallinity and electron-shuttling. To remove residual nitrate from

synthesis, all Fh suspensions were dialyzed (6 kDa; ZelluTrans T2, Roth, Germany) against ultrapure water.

Analyses

The electron-accepting capacity of HA and efOM, i.e., the number of electrons transferred to the redox-active constituents in a given aqueous solution, was quantified by mediated electrochemical reduction.[38] In brief, 9 ml glassy carbon cylinders served as both the working electrode and the electrochemical reaction vessel. The reduction potential (E_h) applied to the working electrode was referenced against Ag/AgCl reference electrodes (Bioanalytical Systems Inc., USA), but is reported vs. the standard hydrogen electrode. We used a Pt wire counter electrode in a counter electrode compartment that was separated from the working electrode compartment by a porous glass frit. Both the reference and the counter electrode compartment (filled with 1 mL of 0.1 M KCl, 0.1 M phosphate, pH=7) were lowered into the glassy carbon cylinder (filled with 5.5 mL of 0.1 M KCl, 0.1 M phosphate, pH=7). The mediated electrochemical reduction was conducted at E_h=-0.49 V and used diquat dibromide monohydrate (99.5%, Supelco, USA; final concentration: 0.231 mM) as dissolved electron transfer mediator in the cell. The values for the electron-accepting capacity were determined by integration of the reductive current peaks.[38] Since efOM was exposed

178 to the ambient atmosphere after its discharge from the soil column, we propose that it was re-
179 oxidized by O_2 before being assessed with electrochemical mediated reduction.[39, 40]

180 Powder X-ray diffractograms (XRD) of Fh specimens were obtained from freeze-dried,
181 mortared samples on Si(911) holders (Cu-Kα, 40 kV, 40 mA; D8 Advance, Bruker, Germany).
182 ^{57}Fe Mössbauer spectroscopy was conducted at the Center of Applied Geosciences Tübingen
183 (Eberhard-Karls-University, Germany). Spectra of the freeze-dried Fh samples were collected at
184 room temperature (295 K) and 5 K using a closed-cycle cryostat (Janis Research, USA). Selected
185 samples were measured at 70 K, which was identified in a separate test series as approximate
186 blocking temperature (T_N) of organo-mineral 6-line Fh. Mössbauer spectra were recorded in
187 transmission mode using a constant acceleration drive system (Wissel, Germany) with a source of
188 ^{57}Co in a Rh matrix. The spectra were calibrated against a measurement of α-Fe(0) foil at room
189 temperature and were evaluated with the Recoil software package using Voigt-based fitting.[41] For
190 spectra obtained at room temperature and 5 K, we chose a single site model with two Gaussian
191 components to reflect the spectral asymmetries in the Mössbauer spectra except for three samples,
192 where a two-site model was more appropriate (see discussion). For spectra obtained at 70 K, we
193 chose a two-site model to reflect the coexistence of a magnetically polarized (sextet) and non-

polarized (doublet) component. Iron in efOM-containing soil effluents was analyzed with inductively coupled plasma with optical emission spectrometry (725-ES, Varian). Contents of C, N, S, O and H were determined with an elemental analyzer (Euro EA, EuroVector, Italy).

Microorganisms, media and reduction experiments

Geobacter sulfurreducens strain DSMZ 12127 [42] was obtained from the German Collection of Microorganisms and Cell Cultures (DSMZ, Braunschweig, Germany). The strain was cultivated using standard anaerobic techniques at 303 K in darkness under a N_2/CO_2 (80/20, v/v) atmosphere. The media composition for cell pre-cultivation, cultivation and harvesting is specified elsewhere (Table S3). For the reduction experiments, 1.4 mL of concentrated cell suspension were added to 10 mL low salt mineral medium with trace elements and selenium-tungsten, which contained 11% of the concentration of each compound compared to the (pre-)cultivation medium (Table S3E-H), 11 µM cAMP and 3.85 mM Na-acetate as C- and energy source. The suspensions were buffered at pH~6.8 (TRIS-HCl; Merck). Dialysis of the Fh-containing microbial medium, which was conducted for separate experiments (SpectraPor Biotech CE 20 kDa), revealed that the organic constituents of the microbial medium were not associated with Fh. As opposed to Fh, the organic molecules were completely removed from the dialyzed suspension. Phosphate was omitted in the

media for reduction experiments to avoid the precipitation of vivianite. Stock suspensions with OM-free and organo-mineral Fh were added to achieve 4 mM Fe in each batch. Considering the microbial reduction of 8 mol Fe(III) to oxidize one mole acetate,[1] acetate was added in excess in our reduction experiments. All reduction experiments were performed in triplicates. As positive control, 30 mM Fe(III)-citrate (AppliChem; Germany) was added as electron acceptor instead of Fh. Negative controls were conducted in absence either of Na-acetate or of *G. sulfurreducens* (0.22 µm-filtered cell suspension) and did not show Fe(II) formation (Figure S4). Aqueous Fe(II) was measured in triplicate with the ferrozine assay (560 nm; Wallac 1420 Viktor^3 plate reader, Perkin Elmer, USA).[43]

Quantification of rates and extents of microbial Fe(III) reduction

We applied a pseudo 1st order rate equation (Eq.1) to describe the observed non-linear increase of Fe(II) according to:

$$\frac{\partial c(t)}{\partial t} = k \times \left(c_{MAX} - c(t)\right) \quad \text{(Eq.1)}$$

where $c(t)$ is the Fe(II)-concentration (mM) at time t (h), k is the rate constant (h^{-1}), and c_{MAX} is the Fe(II) concentration (mM), to which $c(t)$ converged during the reduction experiments. We solved Eq.1 assuming $c(t_0)=c_{INIT}$, i.e. the Fe(II) concentration at the start of the experiment. c_{INIT},

226 c_{MAX}, and k were fitted against measured Fe(II) concentrations using the Levenberg-Marquardt
227 algorithm for local optimization.[44] We calculated the 0.95-confidence interval of each fitted
228 parameter to compute the confidence interval of the predicted Fe(II) concentrations. Assuming
229 that Fe(II) production is exclusively coupled to Fh consumption, the half-life of Fh ($T_{1/2}$; h)
230 converging to the concentration of residual (non-reducible) Fh was calculated according to Eq.2.

231 $$T_{1/2} = \frac{ln2}{k} \quad \text{(Eq.2)}$$

232 ## RESULTS AND DISCUSSION

233 ### Properties of effluent organic matter from anoxic topsoil (efOM)

234 Humic acids commonly facilitate the microbial reduction of iron (oxyhydr-) oxides, but the
235 extent to which these findings apply to redoximorphic soils remains unclear. Compared to HA
236 from anoxic groundwater, efOM from our soil column experiments reproducibly exhibited a very
237 different chemical composition. The combined masses of C, N, S, O and H accounted for only
238 79±3% of the mass of efOM, compared to ~91% of the mass of HA (Table 1). The remaining mass
239 of efOM is attributed to the abundance of residual nano-aggregated Fe-OM coprecipitates (Figure
240 S2). These precipitates contain poorly-crystalline Fh [25] and probably formed from Fe(II), which

241 resided in the effluent despite dialysis, due to the increase in effluent pH from 0.9 (acidified with
242 0.25 M HCl) to 4.8 after dialysis against ultrapure water. Assuming that Fe present in the dialyzed
243 effluent was present as Fh,[25] the mass of Fh must have accounted for 21±2% in efOM (Table 1),
244 thereby closing the gap in efOM mass balance. The C/N ratios were clearly lower in efOM than in
245 HA. Assuming that amides are the dominant chemical form of nitrogen in OM from soils and
246 sediments,[17] the relative content of peptides was likely higher in efOM than in HA, which was also
247 revealed by the corresponding ^{13}C-NMR spectra (Figure S5). Absorbance bands characteristic of
248 proteins and polysaccharides were more pronounced in the FTIR spectra of efOM and of organo-
249 mineral Fh with efOM than in the spectra of HA and HA-associated Fh (Figure S6). efOM also
250 exhibited a comparably low C/S ratio (Table 1). Considering that efOM was mobilized under
251 sulfate-reducing conditions,[26] it is possible that the elevated S content of efOM resulted from
252 reactions of H_2S with organic molecules.[45, 46] Since HA was obtained from anoxic groundwater,[33]
253 the C/S ratio was also low in comparison to ancillary OM references, which were retrieved under
254 oxic conditions (i.e., water-extractable OM; Table S4).

255 The electron-accepting capacity (EAC) of efOM was dominated by Fe(III) (Table 1), consistent
256 with complete reduction of Fe(III) in the residual, low-crystalline Fe-OM coprecipitates [25] as

257 previously demonstrated for ferrihydrite.[47] This conclusion was based on a close-to-exact match
258 between the number of electrons accepted by the dialyzed effluents and their molar Fe
259 concentrations (Table 1). We exclude the presence of Fe(II) in the dialyzed effluent because Fe(II)
260 is expected to rapidly oxidize to Fe(III) after exposing the effluent to ambient air.[25] Good
261 agreement between EAC values and molar Fe(III) contents implies that organic molecules in efOM
262 did not significantly contribute to the measured EAC values (EAC_{OM} in Table 1), likely reflecting
263 the absence (or very low concentration) of quinones and other reducible organic moieties in
264 efOM.[48] We evaluated the possibility of effluent Fe(III) concentration having masked otherwise
265 detectable contributions of reducible moieties in the efOM to EAC: if the efOM had exhibited an
266 EAC representative of terrestrial HA (1.5 mmol e^- (g OM)$^{-1}$) or of terrestrial fulvic acids (0.8 mmol
267 e^- (g OM)$^{-1}$),[48] these moieties would have increased the measured EAC values by 56±5% or
268 30±3%, respectively. Such contributions by organic moieties in efOM would have been readily
269 detectable by mediated electrochemical reduction. The absence of OM-mediated EAC was
270 generally reproduced for efOM from an ancillary anoxic topsoil ($efOM_{Ap}$[1] in Table S4).
271 However, the organic molecules in its independent replicate ($efOM_{Ap}$[2]) exhibited a small EAC,
272 which was nevertheless clearly below our (Table S4) and reported EAC values [48, 49] for humic

273 substances and batch water extracts from organic surface layers. As opposed to efOM, EAC values
274 of HA were dominated by organic redox-active moieties (Table 1).

275 We ascertain that the EAC of humic substances (and water-extractable OM) is significantly
276 higher than the EAC of OM that is likely available at anoxic-oxic interfaces in redoximorphic
277 soils, where electron-shuttling might be a particularly important process. Based on the measured
278 EAC values, we would therefore expect increased microbial Fe(III) reduction rates with increasing
279 amounts of HA, while efOM may rather passivate the Fh aggregate surface for electron uptake and
280 thereby slow down Fe(III) reduction.

281 **Effect of efOM on the mineral properties of organo-mineral Fh**

282 Besides (not) mediating electron transfers, OM may affect the microbial Fe(III) reduction by
283 altering the crystallinity of the iron (oxyhydr-)oxides in organo-mineral associations.[23, 49] In our
284 study, the XRD patterns indicated that all syntheses produced 6-line Fh, irrespectively of whether
285 they were performed in the absence or presence of HA or efOM (Figure 1). Considering the
286 reflection width, we observed no consistent change in the long-range ordering of the Fh
287 crystallites. FTIR spectroscopy confirmed that all syntheses produced 6-line Fh (Figure S6). HA-
288 characteristic bands increased in the FTIR spectra of Fh-HA (adsorbed/co-precipitated) with

289 increasing initial OC/Fe ratios during the Fh synthesis, consistent with increasing relative OM
290 contents in these specimens.

291 Mössbauer spectroscopy revealed (super)paramagnetic iron phases (doublets) at room
292 temperature and magnetically ordered iron phases at 5 K (sextets, Figure S7). The center shifts in
293 the room temperature spectra ranged between 0.33-0.36 mm s^{-1} (Table S5), which is in agreement
294 with the presence of Fe(III).[50] The center shifts are within the range of reported low-crystalline
295 iron (oxyhydr-)oxides, which either reacted with efOM [25] or water-extractable OM [10] or were
296 formed by redox cycles in tropical soils.[51] Moreover, center shifts did not reveal a consistent trend
297 for Fh associated with HA or efOM via adsorption or coprecipitation at variable OM loadings.
298 Two Gaussian components were required to account for the asymmetry in the doublets and sextets,
299 except for three spectra recorded at room temperature (OM-free Fh; Fh with adsorbed HA and
300 with adsorbed efOM), where an additional component (collapsed sextet) was required to obtain
301 physically meaningful fits (Figure S7; Table S5). This could indicate an incipient magnetic
302 ordering already at room temperature, which may point to the presence of goethite in these
303 synthesized materials. If so, the relative contribution of goethite would be very low considering
304 the absence of goethite-specific reflections and bands in the XRD patterns (Figure 1) and FTIR

spectra (Figure S6), respectively. The quadrupole splitting (ΔE_Q) contains the most information on the intraparticle atomic order, which can be extracted from a Mössbauer spectrum [52, 53] and is influenced by interactions of iron with other atoms in the mineral lattice.[54] Higher values of ΔE_Q correspond to a higher degree of distortion relative to a perfect polyhedral ligand electric field.[55] Such distortion arises due to the presence of foreign ligands other than O and OH, e.g., OM.[10] Although the mean values of ΔE_Q were consistently higher for organo-mineral Fh compared to OM-free Fh, these –contrary to our expectations– were not consistently shifted towards higher values for Fh coprecipitated with increasing amounts of HA (Table S5). The highest mean value of ΔE_Q was observed for Fh coprecipitated with efOM_B, which, however, was less pronounced in its independent replicate (efOM_A_cop in Table S5). The broad distributions of ΔE_Q were positively skewed with most probable ΔE_Q of ~0.6 mm s^{-1} and a strong tailing up to 1.5-2 mm s^{-1}, with no obvious dependence on the type and amount of added OM and the mode of association with Fh (Figure 2A-B). Shifts in ΔE_Q values towards higher values were previously reported when pure iron (oxyhydr-)oxides were treated with stepwise increased concentrations of organic additives.[10, 56] Therefore, we infer that Mössbauer spectroscopy is generally capable of detecting such an OM-induced distortion of Fh polyhedra. We therefore expect a similar degree of intraparticle order in

all organo-mineral Fh of this study independent of the type and amount of added OM, while the Fh polyhedra in OM-free Fh exhibit a higher degree of atomic order. Mean values of magnetic hyperfine fields (B_{hf}), which were derived from Mössbauer spectra recorded at 5 K, shifted systematically to lower B_{hf} the more HA was coprecipitated with Fh. In contrast, no such decrease was observed for Fh with increasing amounts of adsorbed HA (Table S5). A lower B_{hf} at constant ΔE_Q points to a higher perturbation of crystallite interactions.[57] OM is known to decrease the crystallite interactions due to magnetic dilution.[56, 58] Increased contents of such "foreign" species in the iron precipitates will therefore shift the distributions of B_{hf} to lower values. In our study, two components with the same ΔE_Q and δ, but variable B_{hf}, were applied to fit the asymmetric sextets in the 5 K spectra. The obtained B_{hf}-distributions were negatively skewed and covered a wide range of 41-53 T. According to our expectations, the coprecipitation of Fh with efOM and HA shifted the B_{hf}-distributions to lower values, while this effect was increasingly pronounced with increasing amounts of HA (Figure 2D). In contrast, adsorption of neither efOM nor HA to Fh shifted the B_{hf}-distributions considerably (Figure 2C). Consequently, we assume decreased crystallite interactions in organo-mineral Fh coprecipitated with efOM and HA. This is likely due to the arrangement of OM molecules between Fh crystallites throughout the entire organo-mineral

aggregate. Presumably, this was not the case if the OM molecules were associated with Fh aggregate surfaces via post-aggregation adsorption. If single mineral phases are evaluated, the blocking temperature (T_N) is inversely correlated to the content in impurities [10, 59, 60] and positively correlated to the primary particle size of this Fe phase.[53] We found that T_N was ~70 K for the organo-mineral Fh from this study (Figure S7). At this temperature, the contribution of a magnetically non-polarized component (doublet) was highest for Fh coprecipitated with efOM and HA, followed by Fh adsorbed with efOM and HA, while OM-free Fh was still fully magnetically ordered (Figure 2E, Figure S7). According to the B_{hf}-distributions extracted from the 5 K spectra (Figure 2C-D), this finding was in general agreement with the expected decrease in T_N due to increasing impurities, which had lowered the crystallite interactions particularly in the Fh-efOM and Fh-HA coprecipitates. However, while the B_{hf}-distribution of OM-free Fh (5 K spectra) was nearly identical to those of Fh with adsorbed HA and efOM (Figure 2C), the latter specimens had small, but reproducibly detectable contributions of a magnetically non-polarized component in their 70 K spectra, which was completely absent in OM-free Fh (Figure S7). We cannot therefore exclude that OM also altered the sizes of Fh primary particles (≠ aggregates) besides the perturbation of Fh crystallite interactions. If so, primary particle sizes presumably increased in the

following order according to the individual contributions of the doublet component in the 70 K spectra: Fh_efOM$_{cop}$ < Fh_HA$_{cop}$ << Fh_HA$_{ads}$ ~ Fh_efOM$_{ads}$ << OM-free Fh.

Considering the inverse relation between abiotic reduction rates and Fh primary particle size,[61] we would expect a faster reduction of Fh that is coprecipitated with efOM and HA. Contrary, given the invariable intraparticle atomic order in organo-mineral Fh, we would not expect an influence by the OM type (HA vs. efOM), its relative content, and the mode of association (adsorbed vs. coprecipitated), on microbial Fe(III) reduction rates driven by changes in the crystal order of Fh.

Microbial reduction experiments

The microbial reduction of OM-free Fh was relatively fast (half-life ~33 h), but incomplete, as indicated by final Fe(II) concentrations that accounted for 50-80% of the total provided Fe(III) (c_{MAX} in Figure 3E). The microbial reduction of Fh with adsorbed HA and efOM was consistently slower (k in Figure 3E), which agrees with previous studies showing that OM passivated Fh surfaces.[18, 62] With increasing amounts of adsorbed HA, the microbial reduction accelerated to some extent (Figure 3E). This finding can be rationalized by the beneficial effect of electron-transfer shuttling by HA [33] above a certain threshold value.[9, 12] It was speculated that *Geobacter* does not use external electron shuttles in natural habitats rich in OM and iron (oxyhydr-)oxides [19]

and that external electron-shuttling exerts a minor influence on the reduction of Fe-OM associations.[9] Nevertheless, electron-shuttling improved the reduction of ferric minerals.[33, 63] As revealed by the lack of a substantial electron-accepting capacity, the organic molecules in efOM – as opposed to HA– could not efficiently accept electrons. This finding supports the idea that efOM passivated the Fh surface for electron uptake. As a consequence, the half-lives of Fh with adsorbed efOM were increased by a factor of 4.8±1.2 compared to OM-free Fh, which was clearly higher than the increase observed in treatments with similar amounts of added HA for adsorption to Fh (Figure 3E).

The extent of Fh reduction increased to ~87% of the expected maximum Fe(II) concentration in treatments with the highest addition of HA for adsorption to Fh, which was approximately twice the extent observed for treatments with the lowest addition of HA for adsorption to Fh. If efOM was adsorbed to Fh, complete Fh reduction occurred (Figure 3E). This particular finding contradicts previous studies that reported lower extents of microbial Fe(III) reduction if water-extractable OM and microbial exudates were added to iron (oxyhydr-)oxides.[9] Following the Lewis-Hard-Soft-Acid-Base concept, which can be used to explain the affinity of metal ions to bind to topsoil OM,[64] we resolve and explain the observed sustained microbial Fe(III) reduction

385 with the specific capability of efOM to form complexes with biogenic Fe(II). The scavenging of
386 (biogenic) Fe(II) is known to extend the Fe(III) mineral reduction by attenuating the Fe(II)-induced
387 passivation of mineral surfaces and microbial cells [7, 65] and the Fe(II)-mediated recrystallization of
388 Fh to more stable Fe(III) minerals.[66] Generally, Fe(II) is considered a comparably soft Lewis acid
389 with a low hardness parameter η_A [67] that is effectively complexed by soft Lewis bases. Such soft
390 Lewis bases are organic ligands with N- and S-containing moieties,[68, 69] which are particularly
391 prevalent in anoxic peats [70] and had a higher affinity to Fe(II) than O-containing moieties.[69, 71]
392 Sulfate-reducing conditions very likely increased the abundance of S-containing moieties in efOM
393 and HA from anoxic groundwater (C/S in Table 1) presumably due to the reaction with H_2S.[45, 46]
394 Interestingly, S-containing moieties were less abundant in ancillary OM specimens derived from
395 batch extractions with water (Table S4). Presumably, this water-extractable OM had not
396 encountered distinct anoxic conditions before and during extraction. The complexation of biogenic
397 Fe(II) by HA during microbial Fe(III) reduction is in line with the increasing extents of Fh
398 reduction with increasing amounts of added HA independent on the mode of its association with
399 Fh (Figure 3E).

The fastest microbial reduction was reproducibly observed for Fh that was coprecipitated with efOM, exceeding the rate constant of OM-free Fh by a factor of 1.48±0.04. Compared to HA at similar initial OC/Fe ratios, the reduction was faster by a factor of ~3. The reduction of Fh coprecipitated with efOM was nearly complete (93±3% of the expected maximum Fe(II) concentration), yet less exhaustive than in the treatments with adsorbed efOM, in which Fe(III) was entirely reduced to Fe(II) (Figure 3E). We attribute the more sustained Fe(III) reduction in the latter treatments to the higher relative concentration of efOM, which likely resulted in a higher total capacity to form complexes with biogenic Fe(II) and thus to sustain the microbial Fe(III) reduction.

Besides OM-mediated electron transfer, changes in iron (oxyhydr-)oxide crystallinity, and scavenging of biogenic Fe(II), OM may also affect the aggregation properties of iron (oxyhydr-)oxides.[72, 73] This effect is relevant considering the inverse correlation of Fe(III) reduction by *Geobacter metallireducens* vs. aggregate size.[9] Based on the following observations, we could not find such a relation in our study: i) Initially, OM-free Fh was dispersed and composed of aggregates with sizes mainly <10 nm (Figure S8). However, when exposed to the microbial medium, settling aggregates >1 µm formed, albeit with comparably short half-lives in the reduction

experiments (Figure 3E). ii) The HA-Fh coprecipitates were composed of settling aggregates at all initial OC/Fe ratios but exhibited decreasing half-lives with increasing relative abundance of HA. iii) Fh with adsorbed HA (initial OC/Fe=0.96 mol_C/mol_{Fe}) was partly dispersed ($Fe_{<0.45\ \mu m}/Fe_{TOTAL}$=0.18; data from dynamic light scattering: d_{H1}=56±8 nm and d_{H2}=684±192 nm), but was nevertheless more slowly reduced than the settling aggregates of HA-Fh coprecipitates. Consequently, we could not define a consistent relationship between microbial Fe(III) reduction rates and the actual aggregate sizes of (organo-mineral) Fh.

In summary, mobile OM from anoxic topsoil (efOM) i) accepts electrons to a much lesser extent than HA from anoxic groundwater and water-extractable OM from batch extractions, ii) likely strongly binds Fe(II) involving N and S-containing moieties (like HA from anoxic groundwater), and iii) is incorporated in Fh aggregates, which possibly decreases the Fh primary particle size if coprecipitated with Fh (like HA). This resulted –among all tested Fh specimens– in the reproducibly fastest, and nearly complete, microbial reduction of Fh coprecipitated with efOM.

ENVIRONMENTAL IMPLICATIONS

As indicated by our study, Fe(III)-OM coprecipitates that form at anoxic-oxic interfaces in soils are likely readily and completely reducible by Fe(III)-reducing bacteria. This results from OM inferring with the Fe mineral crystallinity and likely scavenging the potential surface passivator Fe(II), but not from electron-shuttling to mineral Fe(III). This is attributed to the properties of the likely available OM in these environments, which is comparably rich in N- and S-containing moieties, but only has a negligible capacity to accept electrons. An OM-mediated deceleration of the microbial Fe(III) reduction is likely to be expected only in cases when this OM accumulates on the surface of iron (oxyhydr-)oxides; a process that passivates the surface for further electron uptake due to an electron non-conducting layer. Generally, pedogenic Fe(III)-OM coprecipitates were found to become quickly and completely reduced,[76] and other work suggests reducibility is maintained or increased through reduction and oxidation events.[51]

Our work suggests that OM, which is mobile in anoxic soil regions, may contain much fewer electron-accepting moieties than previously studied OM specimens. This finding is restricted to mobile OM and excludes solid-phase OM, which has a composition different from efOM [16] and was previously shown to contain redox-active moieties both in wetlands [77] and freshwater sediments.[78] However, electron-shuttling by OM and thus OM-enhanced microbial reduction of

446 mineral Fe(III),[8] relies on mobile electron acceptors in the OM *sensu stricto*. Colloidal iron
447 (oxyhydr-)oxides could principally act as alternative electron shuttles at anoxic-oxic interfaces in
448 redoximorphic soils. However, it was shown that these Fe(III)-rich aggregates can remain
449 colloidally stable if formed in soil effluents outside of soils,[25] but are likely to be completely
450 immobilized if precipitated at anoxic-oxic interfaces within soils.[26] Consequently, we propose that
451 neither Fe(III)-OM coprecipitates nor dissolved OM are likely effective electron shuttles in
452 redoximorphic soils due to their immobility or negligible electron-accepting capacities,
453 respectively.

454 Microbial processing of efOM (i.e., its oxidation) will likely affect its functionality, which was
455 not considered in the experimental design of this study. In our study, acetate was added in excess
456 and was likely preferred over efOM or HA as carbon and energy source by *G. sulfurreducens*
457 during the incubations.[79] Furthermore, autochthonous microbial communities –unlike *Geobacter*–[6]
458 might produce endogenous electron-shuttling compounds, which could compensate for the lack
459 (or low abundance) of electron-accepting moieties in efOM. Finally, flow and transport processes
460 along variable gradients are prominent in soils and aquifers and tremendously affect the removal
461 of biogenic Fe(II) and therefore increase the extent of microbial iron (oxyhydr-)oxide reduction

462 and associated bacterial growth.[80] The sustaining of the microbial Fe(III) reduction by efOM-
463 mediated Fe(II)-complexation might therefore be superimposed by advective flow in natural
464 porous media.

465 ASSOCIATED CONTENT

466 Supporting Information.

467 Contains details on i) the used topsoil material, ii) the design of the soil column experiment and
468 the microbial reduction experiments, iii) the efOM (^{13}C-NMR spectra, FTIR spectra, XRD
469 patterns), iv) the properties of ancillary OM specimens for comparison purposes, v) the measured
470 Mössbauer spectra and corresponding fits, and vi) the aggregate properties of OM-free Fh.

471 ACKNOWLEDGEMENTS

472 We thank K. Eusterhues for providing water-extractable OM and M. Steffens for ^{13}C-NMR
473 spectroscopy. We also thank the reviewers for their valuable comments and suggestions.

REFERENCES

1. Lovley, D. R.; Phillips, E. J. P. Novel mode of microbial energy-metabolism - Organic carbon oxidation coupled to dissimilatory reduction of iron or manganese. *Appl. Environ. Microbiol.* **1988**, *54*, 1472-1480; DOI 10.1128/AEM.54.6.1472-1480.1988.
2. Weber, K. A.; Achenbach, L. A.; Coates, J. D. Microorganisms pumping iron: anaerobic microbial iron oxidation and reduction. *Nat. Rev. Microbiol.* **2006**, *4*, 752-764; DOI 10.1038/nrmicro1490.
3. LaRowe, D. E.; Van Cappellen, P. Degradation of natural organic matter: A thermodynamic analysis. *Geochim. Cosmochim. Acta* **2011**, *75*, 2030-2042; DOI 10.1016/j.gca.2011.01.020.
4. Chen, C. M.; Hall, S. J.; Coward, E.; Thompson, A. Iron-mediated organic matter decomposition in humid soils can counteract protection. *Nat. Comm.* **2020**, *11*, 2255; DOI 10.1038/s41467-020-16071-5.
5. Boye, K.; Noel, V.; Tfaily, M. M.; Bone, S. E.; Williams, K. H.; Bargar, J. R.; Fendorf, S. Thermodynamically controlled preservation of organic carbon in floodplains. *Nat. Geosci.* **2017**, *10*, 415-419; DOI 10.1038/ngeo2940.
6. Nevin, K. P.; Lovley, D. R. Mechanisms for accessing insoluble Fe(III) oxide during dissimilatory Fe(III) reduction by *Geothrix fermentans*. *Appl. Environ. Microbiol.* **2002**, *68*, 2294-2299; DOI 10.1128/aem.68.5.2294-2299.2002.
7. Roden, E. E.; Urrutia, M. M. Ferrous iron removal promotes microbial reduction of crystalline iron(III) oxides. *Environ. Sci. Technol.* **1999**, *33*, 1847-1853; DOI 10.1021/es9809859.
8. Lovley, D. R.; Coates, J. D.; Blunt-Harris, E. L.; Phillips, E. J. P.; Woodward, J. C. Humic substances as electron acceptors for microbial respiration. *Nature* **1996**, *382*, 445; DOI 10.1038/382445a0.
9. Poggenburg, C.; Mikutta, R.; Schippers, A.; Dohrmann, R.; Guggenberger, G. Impact of natural organic matter coatings on the microbial reduction of iron oxides. *Geochim. Cosmochim. Acta* **2018**, *224*, 223-248; DOI 10.1016/j.gca.2018.01.004.
10. Eusterhues, K.; Wagner, F. E.; Hausler, W.; Hanzlik, M.; Knicker, H.; Totsche, K. U.; Kögel-Knabner, I.; Schwertmann, U. Characterization of ferrihydrite-soil organic matter coprecipitates by X-ray diffraction and Mössbauer spectroscopy. *Environ. Sci. Technol.* **2008**, *42*, 7891-7897; DOI 10.1021/es800881w.

11. Mikutta, C.; Kretzschmar, R. Synthetic coprecipitates of exopolysaccharides and ferrihydrite. Part II: Siderophore-promoted dissolution. *Geochim. Cosmochim. Acta* **2008**, *72*, 1128-1142; DOI 10.1016/j.gca.2007.11.034.
12. Amstaetter, K.; Borch, T.; Kappler, A. Influence of humic acid imposed changes of ferrihydrite aggregation on microbial Fe(III) reduction. *Geochim. Cosmochim. Acta* **2012**, *85*, 326-341; DOI 10.1016/j.gca.2012.02.003.
13. Cutting, R. S.; Coker, V. S.; Fellowes, J. W.; Lloyd, J. R.; Vaughan, D. J. Mineralogical and morphological constraints on the reduction of Fe(III) minerals by *Geobacter sulfurreducens*. *Geochim. Cosmochim. Acta* **2009**, *73*, 4004-4022; DOI 10.1016/j.gca.2009.04.009.
14. Bonneville, S.; Van Cappellen, P.; Behrends, T. Microbial reduction of iron(III) oxyhydroxides: effects of mineral solubility and availability. *Chem. Geol.* **2004**, *212*, 255-268; DOI
15. Bosch, J.; Heister, K.; Hofmann, T.; Meckenstock, R. U. Nanosized iron oxide colloids strongly enhance microbial iron reduction. *Appl. Environ. Microbiol.* **2010**, *76*, 184-189; DOI 10.1128/aem.00417-09.
16. Kleber, M.; Johnson, M. G. Advances in understanding the molecular structure of soil organic matter: Implications for interactions in the environment. In *Advances in Agronomy 106*; Sparks, D. L., Ed.; Academic Press: San Diego, 2010; Vol. 106, pp 77-142.
17. Lehmann, J.; Kleber, M. The contentious nature of soil organic matter. *Nature* **2015**, *528*, 60-68; DOI 10.1038/nature16069.
18. Eusterhues, K.; Hädrich, A.; Neidhardt, J.; Küsel, K.; Keller, T. F.; Jandt, K. D.; Totsche, K. U. Reduction of ferrihydrite with adsorbed and coprecipitated organic matter: microbial reduction by *Geobacter bremensis* vs. abiotic reduction by Na-dithionite. *Biogeosciences* **2014**, *11*, 4953-4966; DOI 10.5194/bg-11-4953-2014.
19. Cooper, R. E.; Eusterhues, K.; Wegner, C. E.; Totsche, K. U.; Küsel, K. Ferrihydrite-associated organic matter (OM) stimulates reduction by *Shewanella oneidensis* MR-1 and a complex microbial consortia. *Biogeosciences* **2017**, *14*, 5171-5188; DOI 10.5194/bg-14-5171-2017.
20. Poggenburg, C.; Mikutta, R.; Sander, M.; Schippers, A.; Marchanka, A.; Dohrmann, R.; Guggenberger, G. Microbial reduction of ferrihydrite-organic matter coprecipitates by *Shewanella putrefaciens* and *Geobacter metallireducens* in comparison to mediated

electrochemical reduction. *Chemical Geology* **2016**, *447*, 133-147; DOI 10.1016/j.chemgeo.2016.09.031.

21. Zsolnay, A. Dissolved organic matter: artefacts, definitions, and functions. *Geoderma* **2003**, *113*, 187-209; DOI 10.1016/50016-7061(02)00361-0.
22. Rennert, T.; Gockel, K. F.; Mansfeldt, T. Extraction of water-soluble organic matter from mineral horizons of forest soils. *J. Plant Nutr. Soil Sci.* **2007**, *170*, 514-521; DOI 10.1002/jpln.200625099.
23. Chen, C. M.; Meile, C.; Wilmoth, J.; Barcellos, D.; Thompson, A. Influence of pO(2) on iron redox cycling and anaerobic organic carbon mineralization in a humid tropical forest soil. *Environ. Sci. Technol.* **2018**, *52*, 7709-7719; DOI 10.1021/acs.est.8b01368.
24. Gu, B. H.; Schmitt, J.; Chen, Z. H.; Liang, L. Y.; McCarthy, J. F. Adsorption and desorption of natural organic matter on iron oxide - Mechanisms and models. *Environ. Sci. Technol.* **1994**, *28*, 38-46; DOI 10.1021/es00050a007.
25. Fritzsche, A.; Schröder, C.; Wieczorek, A. K.; Handel, M.; Ritschel, T.; Totsche, K. U. Structure and composition of Fe-OM co-precipitates that form in soil-derived solutions. *Geochim. Cosmochim. Acta* **2015**, *169*, 167-183; DOI 10.1016/j.gca.2015.07.041.
26. Fritzsche, A.; Pagels, B.; Totsche, K. U. The composition of mobile matter in a floodplain topsoil: A comparative study with soil columns and field lysimeters. *J. Plant Nutr. Soil Sci.* **2016**, *179*, 18-28; DOI 10.1002/jpln.201500169.
27. Wehrer, M.; Totsche, K. U. Detection of non-equilibrium contaminant release in soil columns: Delineation of experimental conditions by numerical simulations. *J. Plant Nutr. Soil Sci.* **2003**, *166*, 475-483; DOI 10.1002/jpln.200321095.
28. IUSS Working Group WRB. *World reference base for soil resources 2014, update 2015, International soil classification system for naming soils and creating legends for soil maps*. FAO: Rome, Italy, 2015.
29. Eusterhues, K.; Rennert, T.; Knicker, H.; Kögel-Knabner, I.; Totsche, K. U.; Schwertmann, U. Fractionation of organic matter due to reaction with ferrihydrite: Coprecipitation versus adsorption. *Environ. Sci. Technol.* **2011**, *45*, 527-533; DOI 10.1021/es1023898.
30. Kalbitz, K.; Solinger, S.; Park, J. H.; Michalzik, B.; Matzner, E. Controls on the dynamics of dissolved organic matter in soils: A review. *Soil Sci.* **2000**, *165*, 277-304; DOI 10.1097/00010694-200004000-00001.

31. Singer, P. C.; Stumm, W. Acidic mine drainage. Rate-determining step. *Science* **1970**, *167*, 1121-1123; DOI 10.1126/science.167.3921.1121.
32. Borisover, M.; Lordian, A.; Levy, G. J. Water-extractable soil organic matter characterization by chromophoric indicators: Effects of soil type and irrigation water quality. *Geoderma* **2012**, *179*, 28-37; DOI 10.1016/j.geoderma.2012.02.019.
33. Wolf, M.; Kappler, A.; Jiang, J.; Meckenstock, R. U. Effects of humic substances and quinones at low concentrations on ferrihydrite reduction by *Geobacter metallireducens*. *Environ. Sci. Technol.* **2009**, *43*, 5679-5685; DOI 10.1021/es803647r.
34. Aiken, G. R.; Thurman, E. M.; Malcolm, R. L.; Walton, H. F. Comparison of XAD macroporous resins for the concentration of fulvic acid from aqueous solution. *Anal. Chem.* **1979**, *51*, 1799-1803; DOI 10.1021/ac50047a044.
35. Schwertmann, U.; Cornell, R. M. *Iron Oxides in the Laboratory*. 2nd ed.; WILEY-VCH Verlag GmbH: Weinheim, Germany, 2000.
36. Chen, C. M.; Dynes, J. J.; Wang, J.; Sparks, D. L. Properties of Fe-organic matter associations via coprecipitation versus adsorption. *Environ. Sci. Technol.* **2014**, *48*, 13751-13759; DOI 10.1021/es503669u.
37. Braunschweig, J.; Klier, C.; Schröder, C.; Handel, M.; Bosch, J.; Totsche, K. U.; Meckenstock, R. U. Citrate influences microbial Fe hydroxide reduction via a dissolution disaggregation mechanism. *Geochim. Cosmochim. Acta* **2014**, *139*, 434-446; DOI 10.1016/j.gca.2014.05.006.
38. Klüpfel, L.; Keiluweit, M.; Kleber, M.; Sander, M. Redox properties of plant biomass-derived black carbon (biochar). *Environ. Sci. Technol.* **2014**, *48*, 5601-5611; DOI 10.1021/es500906d.
39. Bauer, I.; Kappler, A. Rates and extent of reduction of Fe(III) compounds and O_2 by humic substances. *Environ. Sci. Technol.* **2009**, *43*, 4902-4908; DOI 10.1021/es900179s.
40. Klüpfel, L.; Piepenbrock, A.; Kappler, A.; Sander, M. Humic substances as fully regenerable electron acceptors in recurrently anoxic environments. *Nat. Geosci.* **2014**, *7*, 195-200; DOI 10.1038/ngeo2084.
41. Rancourt, D. G.; Ping, J. Y. Voigt-based methods for arbitrary-shape static hyperfine parameter distributions in Mössbauer spectroscopy. *Nucl. Instrum. Meth. B* **1991**, *58*, 85-97; DOI 10.1016/0168-583x(91)95681-3.
42. Caccavo, F.; Lonergan, D. J.; Lovley, D. R.; Davis, M.; Stolz, J. F.; McInerney, M. J. *Geobacter sulfurreducens* sp. nov., a hydrogen- and acetate oxidizing dissimilatory metal-

598 reducing microorganism. *Appl. Environ. Microbiol.* **1994**, *60*, 3752-3759; DOI
599 10.1128/AEM.60.10.3752-3759.1994.
600 43. Stookey, L. L. Ferrozine - A new spectrophotometric reagent for iron. *Anal. Chem.* **1970**, *42*,
601 779-781; DOI 10.1021/ac60289a016.
602 44. Marquardt, D. W. An algorithm for least-squares estimation of nonlinear parameters. *SIAM*
603 *J. Appl. Math.* **1963**, *11*, 431-441; DOI 10.1137/0111030.
604 45. Casagrande, D. J.; Idowu, G.; Friedman, A.; Rickert, P.; Siefert, K.; Schlenz, D. H_2S
605 incorporation in coal precursors - Origins of organic sulfur in coal. *Nature* **1979**, *282*, 599-
606 600; DOI 10.1038/282599a0.
607 46. Urban, N. R.; Bayley, S. E.; Eisenreich, S. J. Export of dissolved organic carbon and acidity
608 from peatlands. *Water Resour. Res.* **1989**, *25*, 1619-1628; DOI 10.1029/WR025i007p01619.
609 47. Aeppli, M.; Voegelin, A.; Gorski, C. A.; Hofstetter, T. B.; Sander, M. Mediated
610 electrochemical reduction of iron (oxyhydr-)oxides under defined thermodynamic boundary
611 conditions. *Environ. Sci. Technol.* **2018**, *52*, 560-570; DOI 10.1021/acs.est.7b04411.
612 48. Aeschbacher, M.; Graf, C.; Schwarzenbach, R. P.; Sander, M. Antioxidant properties of humic
613 substances. *Environ. Sci. Technol.* **2012**, *46*, 4916-4925; DOI 10.1021/es300039h.
614 49. Piepenbrock, A.; Schröder, C.; Kappler, A. Electron transfer from humic substances to
615 biogenic and abiogenic Fe(III) oxyhydroxide minerals. *Environ. Sci. Technol.* **2014**, *48*, 1656-
616 1664; DOI 10.1021/es404497h.
617 50. Gütlich, G.; Schröder, C. Mössbauer Spectroscopy. In *Methods in Physical Chemistry*;
618 Schäfer, R.; Schmidt, P. C., Eds.; Wiley-VCH: Weinheim, 2012; pp 351-389.
619 51. Ginn, B.; Meile, C.; Wilmoth, J.; Tang, Y.; Thompson, A. Rapid iron reduction rates are
620 stimulated by high-amplitude redox fluctuations in a tropical forest soil. *Environ. Sci.*
621 *Technol.* **2017**, *51*, 3250-3259; DOI 10.1021/acs.est.6b05709.
622 52. Rancourt, D. G.; Fortin, D.; Pichler, T.; Thibault, P. J.; Lamarche, G.; Morris, R. V.; Mercier,
623 P. H. J. Mineralogy of a natural As-rich hydrous ferric oxide coprecipitate formed by mixing
624 of hydrothermal fluid and seawater: Implications regarding surface complexation and color
625 banding in ferrihydrite deposits. *Am. Miner.* **2001**, *86*, 834-851; DOI
626 53. Rancourt, D. G.; Thibault, P. J.; Mavrocordatos, D.; Lamarche, G. Hydrous ferric oxide
627 precipitation in the presence of nonmetabolizing bacteria: Constraints on the mechanism of a
628 biotic effect. *Geochim. Cosmochim. Acta* **2005**, *69*, 553-577; DOI 10.1016/j.gca.2004.07.018.

54. Rancourt, D. G. Mössbauer spectroscopy in clay science. *Hyperfine Interact.* **1998**, *117*, 3-38; DOI 10.1023/a:1012651628508.
55. Rea, B. A.; Davis, J. A.; Waychunas, G. A. Studies of the reactivity of the ferrihydrite surface by iron isotopic exchange and Mössbauer spectroscopy. *Clay Clay Miner.* **1994**, *42*, 23-34; DOI 10.1346/ccmn.1994.0420104.
56. Mikutta, C.; Mikutta, R.; Bonneville, S.; Wagner, F.; Voegelin, A.; Christl, I.; Kretzschmar, R. Synthetic coprecipitates of exopolysaccharides and ferrihydrite. Part I: Characterization. *Geochim. Cosmochim. Acta* **2008**, *72*, 1111-1127; DOI 10.1016/j.gca.2007.11.035.
57. Morup, S.; Ostenfeld, C. W. On the use of Mössbauer spectroscopy for characterisation of iron oxides and oxyhydroxides in soils. *Hyperfine Interact.* **2001**, *136*, 125-131; DOI 10.1023/A:1015516828586.
58. Cornell, R. M.; Schwertmann, U. *The Iron Oxides*. 2nd ed.; Wiley-VCH: Weinheim, Germany, 2003.
59. Murad, E. Properties and behavior of iron oxides as determined by Mössbauer spectroscopy. In *Iron in Soils and Clay Minerals*; Stucki, J. W.; Goodman, B. A.; Schwertmann, U., Eds.; Springer Netherlands: Dordrecht, 1988; pp 309-350.
60. Murad, E.; Schwertmann, U. The influence of aluminum substitution and crystallinity on the Mössbauer-spectra of goethite. *Clay Minerals* **1983**, *18*, 301-312; DOI 10.1180/claymin.1983.018.3.07.
61. Anschutz, A. J.; Penn, R. L. Reduction of crystalline iron(III) oxyhydroxides using hydroquinone: Influence of phase and particle size. *Geochem. Trans.* **2005**, *6*, 60-66; DOI 10.1063/1.2037887.
62. Swindle, A. L.; Madden, A. S. E.; Cozzarelli, I. M.; Benamara, M. Size-dependent reactivity of magnetite nanoparticles: A field-laboratory comparison. *Environ. Sci. Technol.* **2014**, *48*, 11413-11420; DOI 10.1021/es500172p.
63. MacDonald, L. H.; Moon, H. S.; Jaffé, P. R. The role of biomass, electron shuttles, and ferrous iron in the kinetics of *Geobacter sulfurreducens*-mediated ferrihydrite reduction. *Water Res.* **2011**, *45*, 1049-1062; DOI 10.1016/j.watres.2010.10.017.
64. Stark, P. C.; Rayson, G. D. Comparisons of metal-ion binding to immobilized biogenic materials in a flowing system. *Adv. Environ. Res.* **2000**, *4*, 113-122; DOI 10.1016/S1093-0191(00)00012-5.

65. Royer, R. A.; Burgos, W. D.; Fisher, A. S.; Unz, R. F.; Dempsey, B. A. Enhancement of biological reduction of hematite by electron shuttling and Fe(II) complexation. *Environ. Sci. Technol.* **2002**, *36*, 1939-1946; DOI 10.1021/es011139s.
66. Aeppli, M.; Kaegi, R.; Kretzschmar, R.; Voegelin, A.; Hofstetter, T. B.; Sander, M. Electrochemical analysis of changes in iron oxide reducibility during abiotic ferrihydrite transformation into goethite and magnetite. *Environ. Sci. Technol.* **2019**, *53*, 3568-3578; DOI 10.1021/acs.est.8b07190.
67. Parr, R. G.; Pearson, R. G. Absolute hardness - Companion parameter to absolute electronegativity. *J. Am. Chem. Soc.* **1983**, *105*, 7512-7516; DOI 10.1021/ja00364a005.
68. Pullin, M. J.; Anthony, C.; Maurice, P. A. Effects of iron on the molecular weight distribution, light absorption, and fluorescence properties of natural organic matter. *Environ. Eng. Sci.* **2007**, *24*, 987-997; DOI 10.1089/ees.2006.0040.
69. Harris, W. R. Iron Chemistry. In *Molecular and Cellular Iron Transport*; Templeton, D. M., Ed.; Marcel Dekker, Inc.: New York, 2005; pp 1-40.
70. Bhattacharyya, A.; Schmidt, M. P.; Stavitski, E.; Martinez, C. E. Iron speciation in peats: Chemical and spectroscopic evidence for the co-occurrence of ferric and ferrous iron in organic complexes and mineral precipitates. *Org. Geochem.* **2018**, *115*, 124-137; DOI 10.1016/j.orggeochem.2017.10.012.
71. Jones, A. M.; Collins, R. N.; Rose, J.; Waite, T. D. The effect of silica and natural organic matter on the Fe(II)-catalysed transformation and reactivity of Fe(III) minerals. *Geochim. Cosmochim. Acta* **2009**, *73*, 4409-4422; DOI 10.1016/j.gca.2009.04.025.
72. Narvekar, S. P.; Ritschel, T.; Totsche, K. U. Colloidal stability and mobility of extracellular polymeric substance amended hematite nanoparticles. *Vadose Zone J.* **2017**, *16*, DOI 10.2136/vzj2017.03.0063.
73. Guhra, T.; Ritschel, T.; Totsche, K. U. Formation of mineral-mineral and organo-mineral composite building units from microaggregate-forming materials including microbially produced extracellular polymeric substances. *Europ. J. Soil Sci.* **2019**, *70*, 604-615; DOI 10.1111/ejss.12774.
74. Voegelin, A.; Kaegi, R.; Frommer, J.; Vantelon, D.; Hug, S. J. Effect of phosphate, silicate, and Ca on Fe(III)-precipitates formed in aerated Fe(II)- and As(III)-containing water studied by X-ray absorption spectroscopy. *Geochim. Cosmochim. Acta* **2010**, *74*, 164-186; DOI 10.1016/j.gca.2009.09.020.

75. Hyacinthe, C.; Bonneville, S.; Van Cappellen, P. Effect of sorbed Fe(II) on the initial reduction kinetics of 6-line ferrihydrite and amorphous ferric phosphate by *Shewanella putrefaciens*. *Geomicrobiology J.* **2008**, *25*, 181-192; DOI 10.1080/01490450802081911.
76. Fritzsche, A.; Bosch, J.; Rennert, T.; Heister, K.; Braunschweig, J.; Meckenstock, R. U.; Totsche, K. U. Fast microbial reduction of ferrihydrite colloids from a soil effluent. *Geochim. Cosmochim. Acta* **2012**, *77*, 444-456; DOI 10.1016/j.gca.2011.10.037.
77. Roden, E. E.; Kappler, A.; Bauer, I.; Jiang, J.; Paul, A.; Stoesser, R.; Konishi, H.; Xu, H. F. Extracellular electron transfer through microbial reduction of solid-phase humic substances. *Nat. Geosci.* **2010**, *3*, 417-421; DOI 10.1038/NGEO870.
78. Lau, M. P.; Sander, M.; Gelbrecht, J.; Hupfer, M. Solid phases as important electron acceptors in freshwater organic sediments. *Biogeochemistry* **2015**, *123*, 49-61; DOI 10.1007/s10533-014-0052-5.
79. Glodowska, M.; Stopelli, E.; Schneider, M.; Lightfoot, A.; Rathi, B.; Straub, D.; Patzner, M.; Duyen, V. T.; Berg, M.; Kleindienst, S.; Kappler, A. Role of in situ natural organic matter in mobilizing As during microbial reduction of Fe-III-mineral-bearing aquifer sediments from Hanoi (Vietnam). *Environ. Sci. Technol.* **2020**, *54*, 4149-4159; DOI 10.1021/acs.est.9b07183.
80. Roden, E. E.; Urrutia, M. M.; Mann, C. J. Bacterial reductive dissolution of crystalline Fe(III) oxide in continuous-flow column reactors. *Appl. Environ. Microbiol.* **2000**, *66*, 1062-1065; DOI 10.1128/AEM.66.3.1062-1065.2000.
81. Michel, F. M.; Ehm, L.; Liu, G.; Han, W. Q.; Antao, S. M.; Chupas, P. J.; Lee, P. L.; Knorr, K.; Eulert, H.; Kim, J.; Grey, C. P.; Celestian, A. J.; Gillow, J.; Schoonen, M. A. A.; Strongin, D. R.; Parise, J. B. Similarities in 2-and 6-line ferrihydrite based on pair distribution function analysis of X-ray total scattering. *Chem. Mat.* **2007**, *19*, 1489-1496; DOI 10.1021/cm062585n.
82. Downs, R. T.; Hall-Wallace, M. The American Mineralogist crystal structure database. *Am. Miner.* **2003**, *88*, 247-250

719 **Table 1.** Contents of C, N, S, O, H and ferrihydrite (Fh), and electron-accepting capacities (EAC)
720 of humic acids (HA) from anoxic groundwater and soil effluent organic matter (efOM) from an
721 anoxic topsoil of a floodplain site (Table S1). $_{A/B}$: independent replicates. *Grey values*:
722 Normalization to OC concentrations invalid as EAC was dominated by Fe(III).

sample	C	N	S	O	H	∑	C/N	C/S	Fh[a]	measured EAC		EAC_{OM}[b]
	g kg^{-1}						g g^{-1}		g kg^{-1}	mmol e^- (mol OC)$^{-1}$	mol e^- (mol Fe)$^{-1}$	µmol e^- (g OM)$^{-1}$
HA	537	3.6	16.5[c]	309	44.2	911	149	33		25.6±0.3	124.0±1.6	1134±15
$efOM_A$	302	9.9	14.3[c]	385[d]	47.5[d]	759	31	21	222	*91.1±2.1*	1.01±0.01	27±33
$efOM_B$	339	16.3	16.1[c]	394[d]	47.4[d]	813	21	21	191	*70.5±2.1*	1.02±0.01	42±21

723 [a] estimated from the OC/Fe concentration ratios in the corresponding effluents; assumptions: all Fe bound
724 in 2l-Fh and $M_{2l\text{-}Fh}$ = 195.7 g mol^{-1} ($Fe_2O_3 \bullet 2H_2O$)[81]
725 [b] corrected for contribution of Fe(III) to EAC (assuming Fe_{total} = Fe(III)): EAC_{OM} = (EAC (µmol e^- L^{-1}) -
726 Fe (µmol L^{-1})) / OM (g L^{-1})
727 [c] sulfate detected with ion chromatography → subtracted from total-S
728 [d] includes contributions from coexistent organo-mineral ferrihydrite

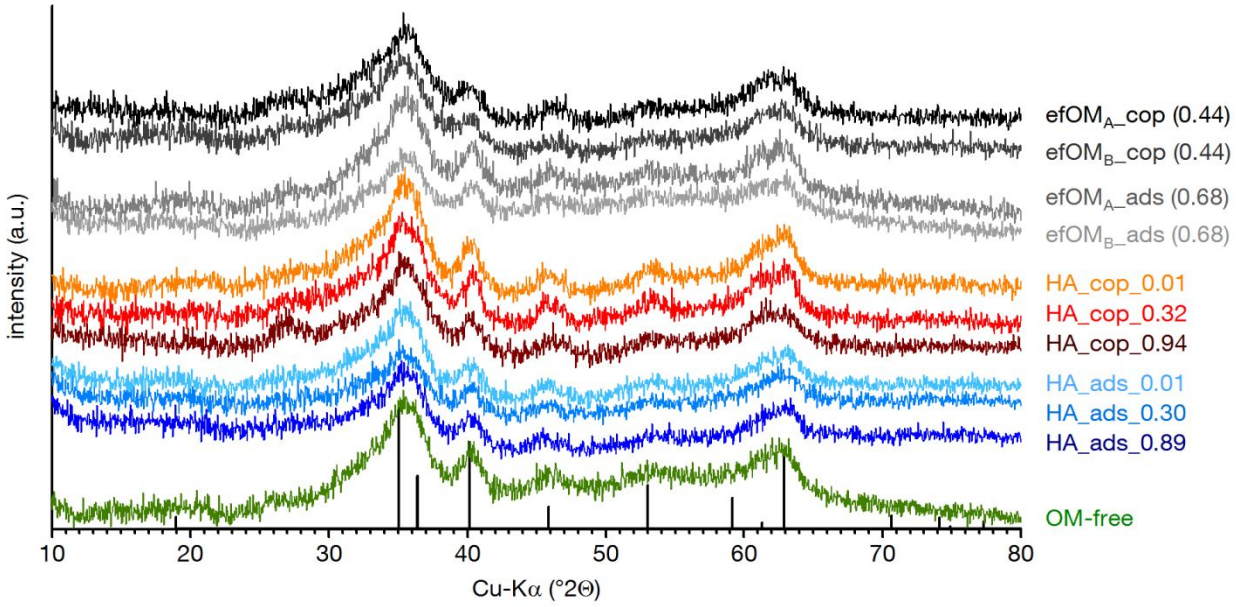

729

730 **Figure 1.** Powder X-ray diffraction patterns of OM-free and organo-mineral ferrihydrite with

731 adsorbed (ads) and coprecipitated (cop) organic matter (OM). efOM: soil effluent OM from an

732 anoxic topsoil of a floodplain site (Table S1). $_{A/B}$: independent replicates. HA: humic acid from

733 anoxic groundwater. The values in the sample name denote the molar OC/Fe ratio, which was set

734 in the corresponding suspension. Black bars depict the powder diffraction reference file of 6-line

735 ferrihydrite.[82]

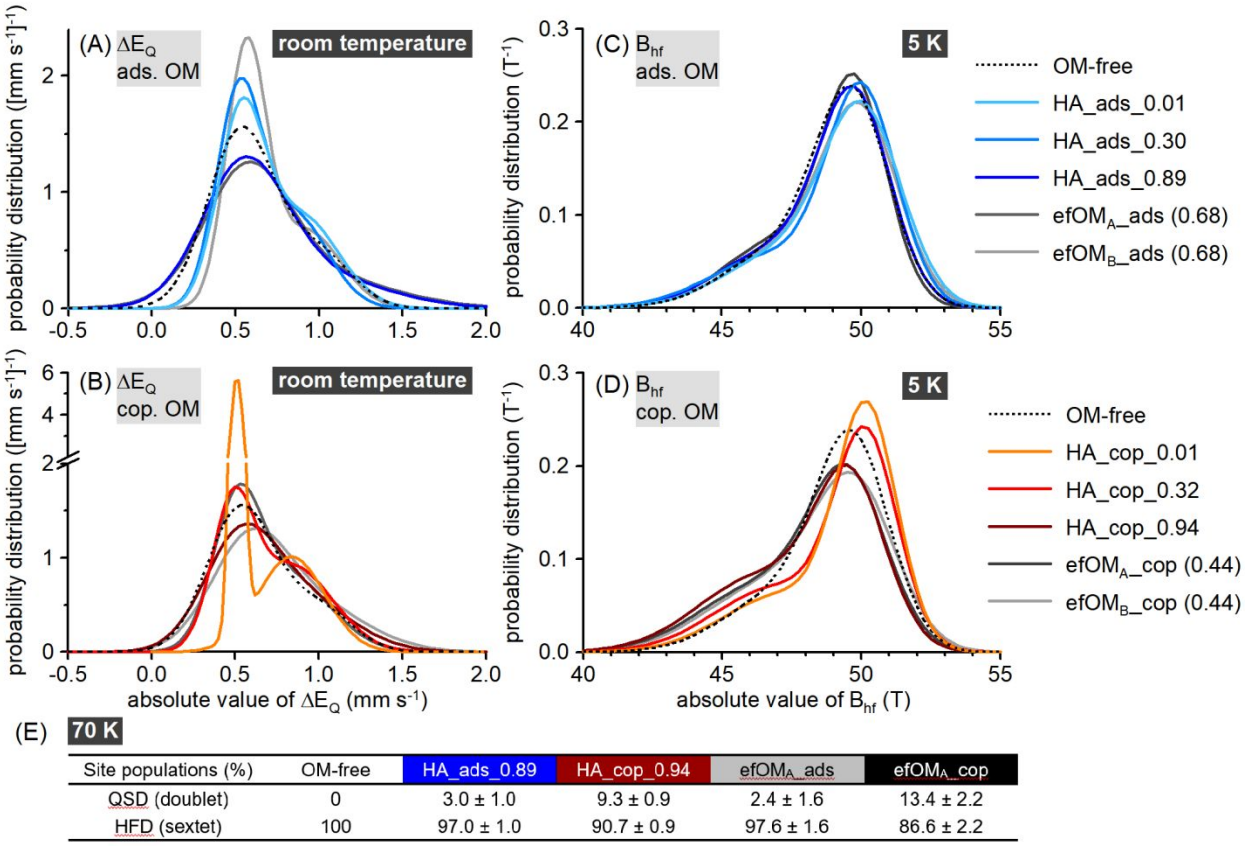

(E) 70 K

Site populations (%)	OM-free	HA_ads_0.89	HA_cop_0.94	efOM$_A$_ads	efOM$_A$_cop
QSD (doublet)	0	3.0 ± 1.0	9.3 ± 0.9	2.4 ± 1.6	13.4 ± 2.2
HFD (sextet)	100	97.0 ± 1.0	90.7 ± 0.9	97.6 ± 1.6	86.6 ± 2.2

Figure 2. Probability distributions of (A, B) the quadrupole splitting (ΔE_Q) and (C, D) of the magnetic hyperfine field (B_{hf}) obtained from the fitted Mössbauer spectra of the OM-free and organo-mineral ferrihydrites recorded at room temperature and 5 K, respectively. (E) Proportion of the doublet- and sextet-component required to fit Mössbauer spectra recorded at 70 K (near blocking temperature; Figure S7, Table S5). ads: adsorbed organic matter (OM). cop: coprecipitated OM. efOM: soil effluent OM from an anoxic topsoil of a floodplain site (Table S1). $_{A/B}$: independent replicates. HA: humic acid from anoxic groundwater. ±: standard deviation. The

744 values in the sample name denote the molar OC/Fe ratio, which was set in the corresponding

745 suspension.

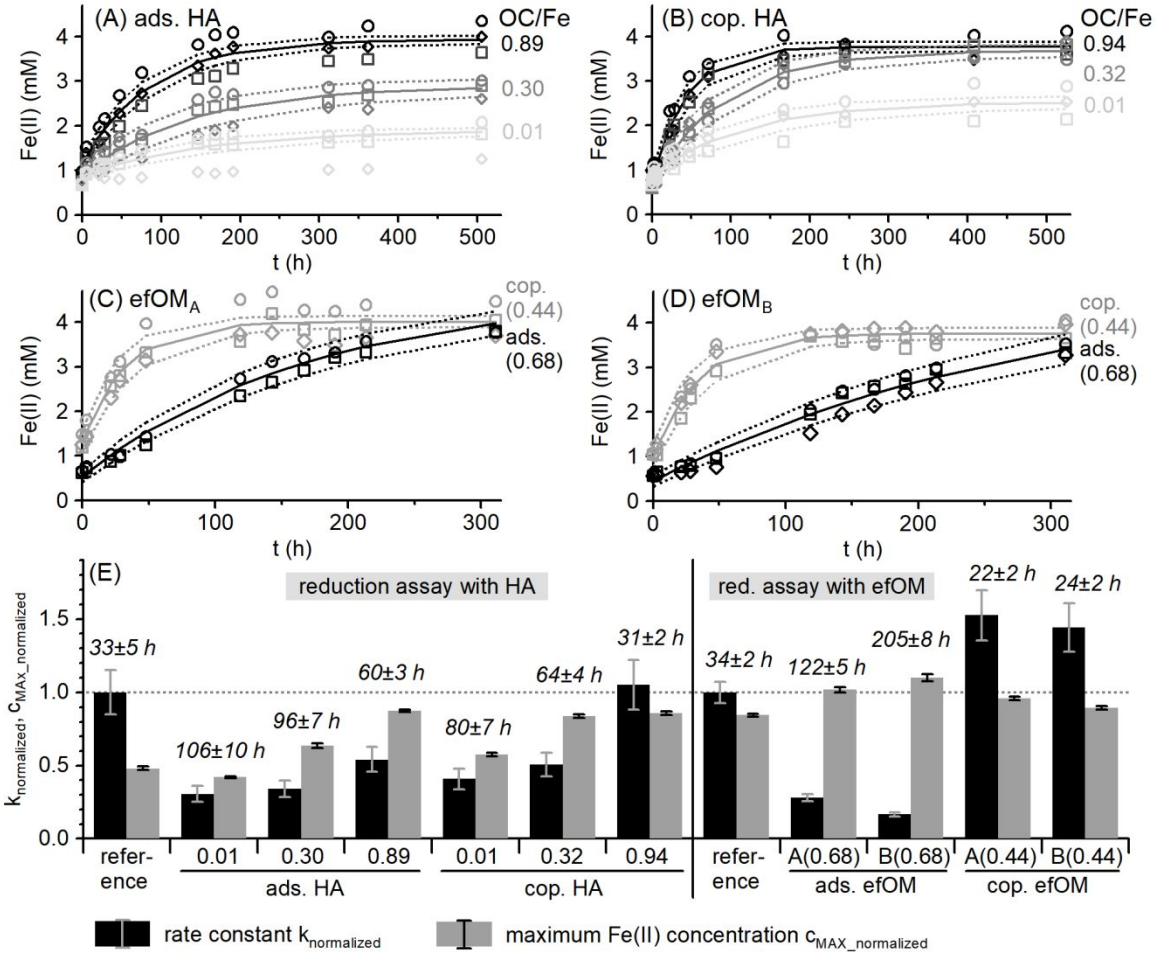

746

747 **Figure 3.** (A-D) Evolution of Fe(II) during the microbial reduction of ferrihydrite (Fh) with

748 adsorbed (ads.) and coprecipitated (cop.) organic matter (OM). HA: humic acid from anoxic

749 groundwater. efOM: soil effluent OM from an anoxic topsoil of a floodplain site (Table S1). $_{A/B}$:

750 independent replicates. Symbols depict mean values of three replicate experiments. Solid / dashed

751 lines depict the prediction of mean Fe(II) concentrations and corresponding 95% confidence
752 intervals, respectively, on basis of fitted *k*, c_{MAX} and c_{INIT} (Eq 1.). (E) Rate constants ($k_{normalized}$),
753 the corresponding half-life of Fh (*italic values*) and maximum Fe(II) concentrations
754 ($c_{MAX\_normalized}$), which parameterize the observed microbial reduction of OM-free (reference) and
755 organo-mineral Fh. The values in the sample description denote the molar OC/Fe ratio, which was
756 set in the corresponding suspension. *k* was normalized to the reduction rate of the corresponding
757 OM-free Fh (reference). c_{MAX} was normalized to the total Fe concentration, which was expected
758 in each treatment (Fe from Fh + *Geobacter* inoculum (Table S3) + residual Fe in efOM (Figure
759 S2)). Error bars and "±" denote the standard error.

760

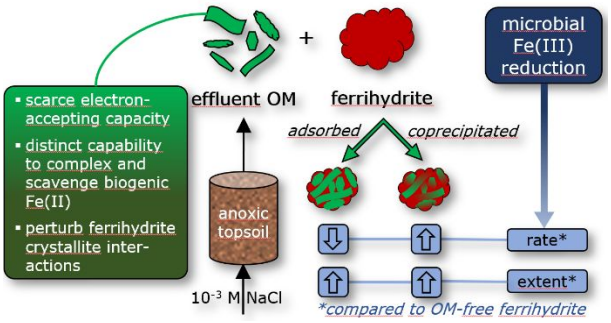

761

762 For Table of Contents Only.